Subsurface Sensing Technologies and Applications, Vol. 6, No. 2, April 2005 (© 2005)
DOI: 10.1007/s11220-005-0010-3
Published Online: August 9, 2005

Joint Interpretation of Geophysical Data for Archaeology: A Case Study

Luciana Orlando*

Department of Idraulica, Trasporti e Strade, 'La Sapienza' University, Via Eudossina, 18, 00184, Rome, Italy

Received October 28, 2004; revised April 23, 2005

Interpret-joints within geophysical data recorded in a complex area where ruins do not outcrop and only earthenware remains within the surficial layer are present. The study area, located in central Italy, consists of Roman, medieval and modern ruins that are included in reworked sediments. The geology is formed by inhomogeneous alluvial sediments (sand and gravel) several meters thick with diamagnetic character. To reduce the ambiguity in the subsurface reconstruction, a joint interpretation of georadar, magnetic and electrical tomography data was performed. The georadar was chosen to reconstruct detailed subsurface features, the electrical tomography to distinguish resistive bodies (stones, voids, etc.) from conductive (cavities filled by clay) and, because of the diamagnetic character of *in situ* sediments, the magnetic method was chosen to detect the earthenware ruins. The geophysical data were controlled by excavation, which detected silos of 1 m in diameter and a concrete layer at a few centimeters from the topographic surface. Time slices in the georadar data allowed us to detect the silos and to define the lateral edge of the concrete layer. Silos were also indirectly detected by the magnetic data because of the earthenware present in the filling sediments. Electrical tomography detected the concrete layer and an ancient anthropogenic surface of few centimeter depths. The study demonstrates that, because the geophysical methods are based on different physical characteristics, they can have different resolution and therefore detect different bodies.

Key Words. Archaeology, georadar, time slice, electrical tomography, magnetic gradient.

1. Introduction

The georadar method allows a high-resolution map of the underlying ground structures to be obtained quickly and at low cost. Both the

*To whom all correspondence should be addressed. Phone: 39-06-44585078; fax: 39-06-44585074; e-mail: luciana.orlando@uniroma1.it

ease of processing a large amount of data economically and its similarity to the seismic reflection method have greatly influenced its rapid evolution. For example, interpretation along vertical profiles is being superceded rapidly by 3D interpretation methods (isosurface, time slices, etc., see [1, 2, 11]). In fact, for today's archeological investigations, it is routine to acquire data along close parallel profiles, so that the archeological site can be analyzed as a 3D cube. In the case of well-preserved structures lying in homogeneous soil, 3D [3–6], is the best representations. However, quite often the archaeological structures are not well preserved and often exist in heterogeneous soil. Furthermore, the archaeological sites may contain different levels; i.e. Roman, medieval and modern ages, all overlapping. In such cases the georadar data are difficult to interpret. To reduce interpretation ambiguity, recourse is made to other geophysical methods such as electrical, magnetic, etc. [7, 8]. In these cases, multiple inversions of data from two or more different methods can be carried out [9], assuming that the structures, which must be, detected produce anomalies in the data. However, this not always occurs; in the most cases different methods detect different elements. In these cases it could be more convenient to process the data separately and to interpret the results jointly. In this way it is possible to reduce the ambiguity in the interpretation and to obtain a better understanding of the subsurface.

We discuss a case study in which several procedures to detect underlying archaeological structures are applied. The joint interpretation was derived by georadar, magnetic and electrical tomography data and the main geophysical anomalies were investigated by excavation. The geo-archaeological complexity of the area (i.e., the inhomogeneous geological formation which can produce a lot of clutter on the georadar data) was the main reason because using several types of geophysical survey were carried out.

2. Geo-archaeological Setting

The study area, located in central Italy, is characterized by an inhomogeneous alluvial formation (sand and gravel) more than 100 m thick and of Plio-Quaternary age. Locally, in the deeper part of the formation, cemented blocks can be found (Fig. 1). In some places a thin layer of humus a few decimeters thick covers this formation. During the last century, the outcropping sediments were strongly mixed by agricultural activity. In the surveyed area (Fig. 2), there are no outcropping Roman ruins, but only a lot of earthenware remains within the surficial layer and the ruins of a medieval Castle. A few kilometers from the study area, archaic and Roman tombs are present.

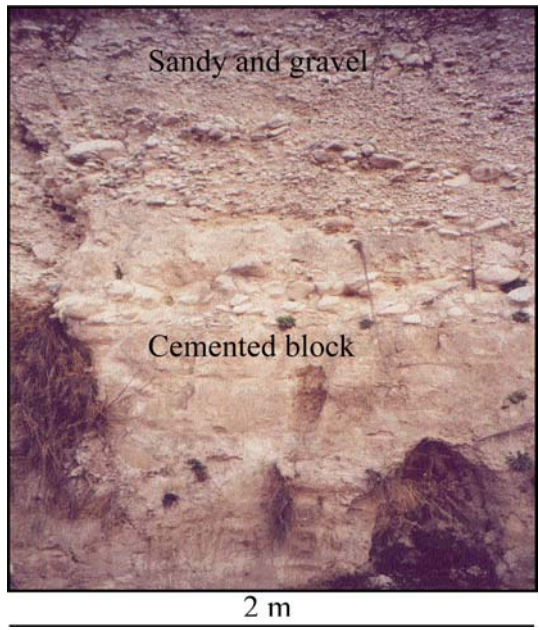

Figure 1. Photo image of the sediments outcropping in the study area. The formation consists of inhomogeneous sand and gravel alluvial deposits more than 100 m thick and are Plio-quaternary in age. On the depth part cemented blocks are present.

Prior to our geophysical surveys, we analyzed the physical characteristics of the sediments and archaeological ruins in order to choose the best geophysical methods to use. Because of the inhomogeneity of the geological formation and the unknown depth of the archaeological ruins, the georadar methods would not be able to reach and to discriminate the anthropogenic structures from the natural ones. Therefore although this method is usually preferred in archaeology, other methods were also planned. The different magnetic character of the sediments (diamagnetic) with respect to that of the earthenware (ferromagnetic) suggested the use of magnetic method. On the hypothesis that archaeological structures, like tombs could be filled by soil, clay, or air, and that structures built from stones could be present in the area, we decided to also use electrical tomography.

The area was chosen on the basis of oral communications that reported that in the past same archaeological finds in age Roman, were performed.

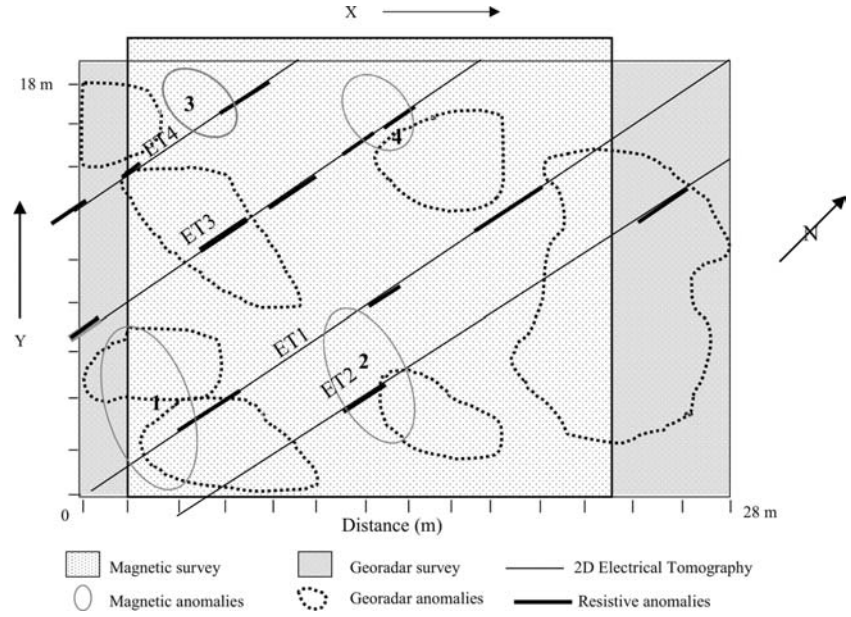

Figure 2. Location of georadar, magnetic and 2D electrical tomography surveys.

3. Geophysical Surveys and Data Processing

3.1. Georadar

3.1.1. Data Acquisition and Processing

An area, 18.5×28 m wide, was surveyed with 50, 100 and 200 MHz antennas in a continuous profiling mode (Fig. 2). The three antennas provided with different resolution and depth of penetration. An example of data acquired with the three different antennas along the same profile is shown in Figure 3. The three pulses have reached similar depths (at more than 100 ns), but with different lateral and vertical resolution. For example, laterally the anomaly A in the 50- and 100-MHz profiles (Fig. 3) appears to be due to a single structure, while the higher resolution 200 MHz antenna shows how the anomaly is the sum of two distinct anomalies. Vertically, the zone B is a better resolved at 200 MHz then at 50 and 100 MHz. Consequently, only the 200 MHz data are discussed here. We also performed common mid point (CMP) profiles with a transmitter-receiver offset increment of 0.1 m. Examples of CMP's acquired with 100 and 200 MHz antennas are shown in Figure 4. The root-mean-square

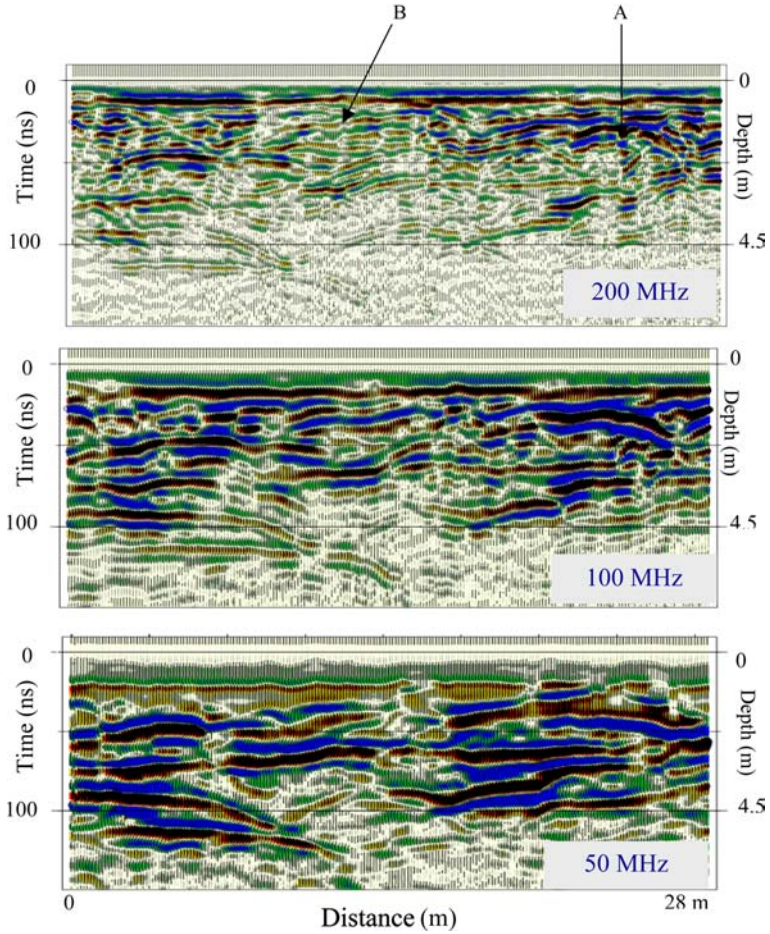

Figure 3. Georadar profiles acquired with 200 MHz (top), 100 MHz (middle) and with 50 MHz (bottom) antennas.

wave velocity of about 0.085–0.09 m/ns was calculated from CMP and diffraction analyses. For the peak pulse frequency of 120–150 MHz at this velocity a wavelength of 1–1.4 m result and a time resolution of 1/2 of wavelength can be hypotheses.

Using the 200 MHz antenna 52 profiles were acquired: 38 profiles spaced 0.5 m in the y-direction and 14 profiles spaced 2 m in the x-direction (Fig. 2). A time window of 500 ns and a sampling rate of 0.8 ns were used during the data acquisition. The antenna position along the profile was obtained with marks every 2 m.

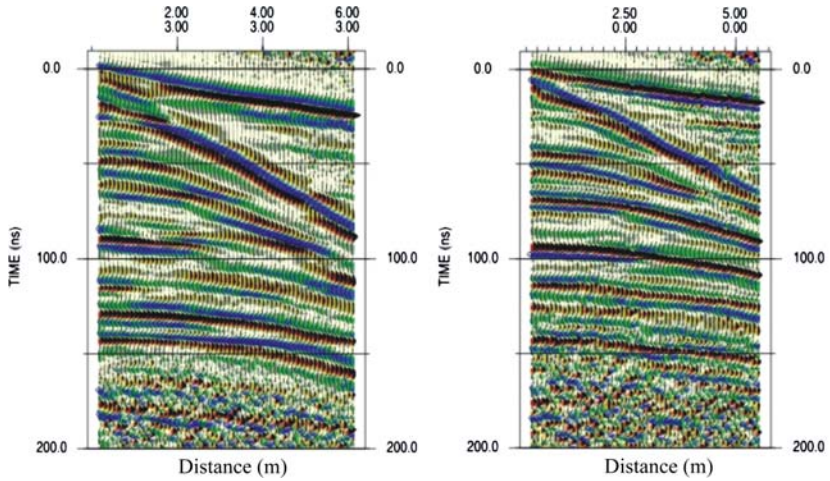

Figure 4. CMP profiles acquired with 100 MHz (left) and 200 MHz (right) antennas. The CMP offset increments were 0.1 m . An root-mean-square electromagnetic velocity between 0.85 and 0.9 cm/ns was estimated on the reflections waves.

We processed the data with time resembling, spatial resembling, time-zero drift removal, pass-band filtering, exponential gain and migration. The time resembling was 0.2 ns and the spatial resembling was obtained between the marks by inserting interpolated traces or by deleting traces. In this way, a spatial sampling of 0.1 m along the profile was obtained. Giving the peak frequency of 120–150 MHz, a pass band Butterworh filter between 60–220 MHz was applied. The migration was based on the 2D F-K algorithm using a constant velocity of 0.09 m/ns. The 38 migrated profiles acquired along the x-direction were used to build a 3D cube. Therefore the 3D cube has a time sampling interval of 2 ns, and a spatial sampling of 0.1 m in the x-direction and 0.5 m in the y-direction.

3.1.2. Data Interpretation

To characterize the anomalies detected by georadar, we analyzed of all of the unmigrated and migrated vertical profiles acquired in the x- and y-directions and horizontal time slices sampled every 2 ns. Because diffraction hyperbolas often better characterize small structures, in the following figures only the unmigrated vertical profiles are shown. The vertical sections show that in the area many anomalies with high reflectivity and located at different depths are present. Some of those anomalies are detected by several profiles, for example the anomaly D in Figure 6 and 7, while others

are only detected by one profile. The zones where the vertical profile have detected the most significant georadar anomalies are shown in Figure 2.

The time slices were difficult to interpret and not all of the detected anomalies were easy to interpret as anthropogenic structures because of their indistinct shape. The main causes of the irregular edge of images on the time slices were probably the low lateral resolution, the non-homogeneous spatial sampling (few centimeters along the profile in the x-direction and $\sim$0.5 m in the y-direction) and the probably poorly preserved geometries of structures.

Starting from the topographic surface the time slices show a highly reflective horizon (indicated with A in Figs. 5–7) that in part is obliterated by the direct wave. This anomaly can be produced by an ancient topographic surface. Below this surface a well-preserved structure (Fig. 6), indicated with E in Figure 5 is present. This anomaly could be due to a tomb. In the time slice at 14 ns (Fig. 5) organized anomalies in the x- and y-directions are clearly evident (B). On the vertical profiles such anomalies appear as in Figure 8. Those anomalies can be interpreted as walls. The time slice at 18 ns (Fig. 5) detects a semi-circular anomaly (C) that in the profile P2 of Figure 6 appear vertically bounded, on the right of anomaly C, more complex and deeper anomalies are present. Anomalies having high reflectivity with no clearly defined shape are detected on the time slices at 32 and 36 ns (indicated by D in Fig. 5). The analysis of vertical profiles (Figs. 7 and 8) allows us to characterize this anomaly as being due to a complex anthropogenic structure.

The combined analyses of the time slices and the vertical profiles have shown that the first 60–70 ns is an anthropogenic level probably characterized by a remade structure that could be associated with different kind of structures (walls, tombs, etc.).

3.1.3. Magnetic Survey

The magnetic survey was carried out using a proton gradiometer instrument with 0.1 nanoTesla (nT) sensitivity. The data were acquired on an area of 19×21 m sampled on a grid of 0.5 m (Fig. 2). A variance less than 0.045 nT, calculated on the repeated measures on the same point, is obtained. We processed the data with the despiking and a circular weighted spatial filter with 1 m in diameter. The magnetic data (Fig. 9) show gradients varying from -2 to 3 nT. The most important anomalies are circular and are located in the South corner of the area (Fig. 9). Because of the diamagnetic character of the geological formation and the presence of earthenware remains within the surficial layer the anomalies are interpreted as caused by anthropogenic remains. The main magnetic anomalies are reported in Figure 2.

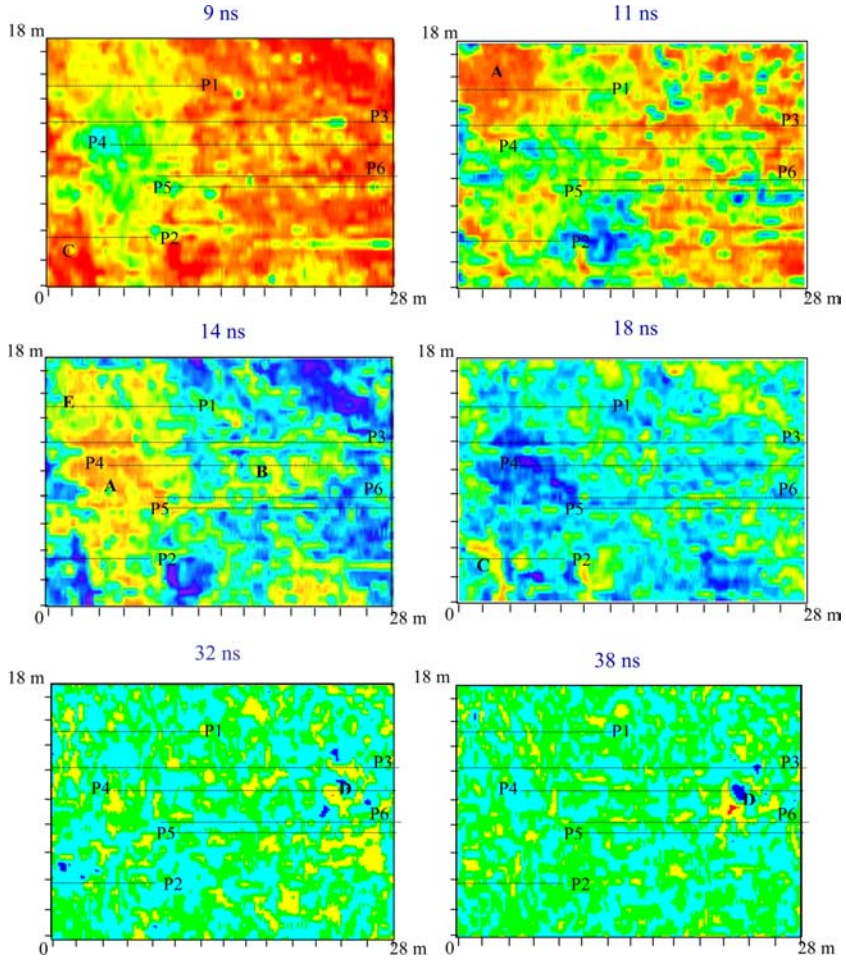

Figure 5. Georadar time slices. The letters indicate the main anomalies and the dotted lines refer to the profiles shown in Figures 6–8.

3.1.4. Electrical Tomography

We acquired 2D electrical dipole–dipole tomography using a Sting instrument equipped with 28 electrodes spaced 0.5 m. The locations of profiles are shown in Figure 2. The profiles ET1, ET2 and ET3 were acquired using the roll-along method with an offset of 7.5 m.

We inverted the data with the Loke program [10] using finite differences. The inverted profiles (Fig. 10) show a surficial layer a few

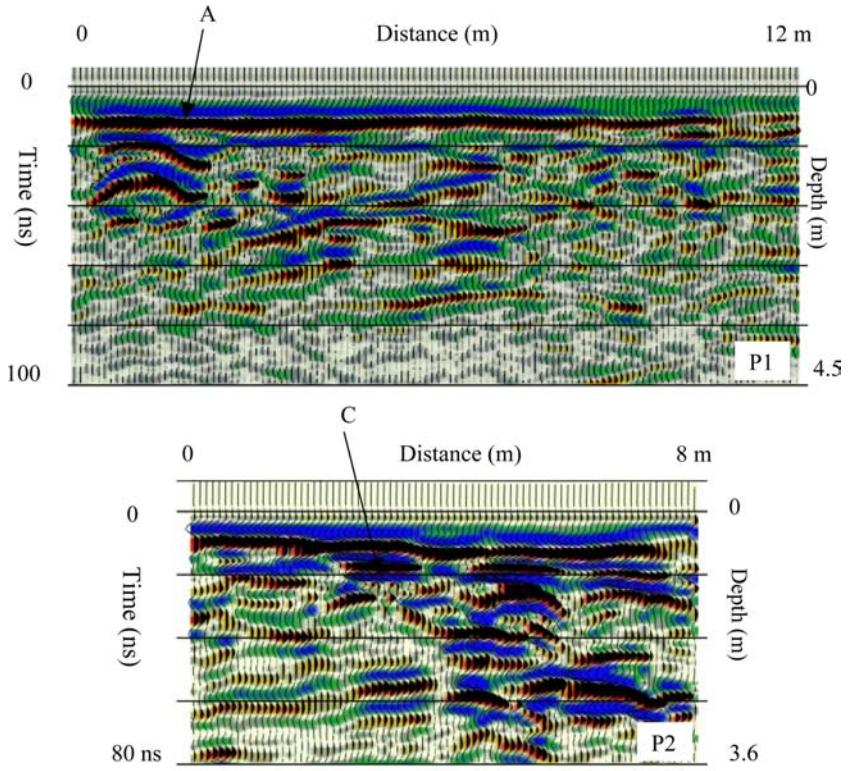

Figure 6. Unmigrated georadar profiles. For locations See Figure 5. The main anomalies are indicated with capital letters.

decimeters thick with a resistivity of 60–80 Ωm, which overlies a zone less then 1 m thick, in which anomalies with resistivity greater then 2000 Ωm are present. The deepest zone is characterized by a resistivity of about 80 Ωm. The high resistive anomalies of middle zone were associated with the anthropogenic structures made by lithoid or cemented structures. The main resistive anomalies are reported in Figure 2.

3.2. Joint Interpretation of the Geophysical Data

The joint interpretation of the multiple data sets does not give a consistent local overlapping of the anomalies (Fig. 2). A full overlap obtained with the three different methods is obtained in area 1, 2 and in parts of 3 and 4. Starting from the consideration that the study area is characterized by diamagnetic formation, formed by heterogeneous material

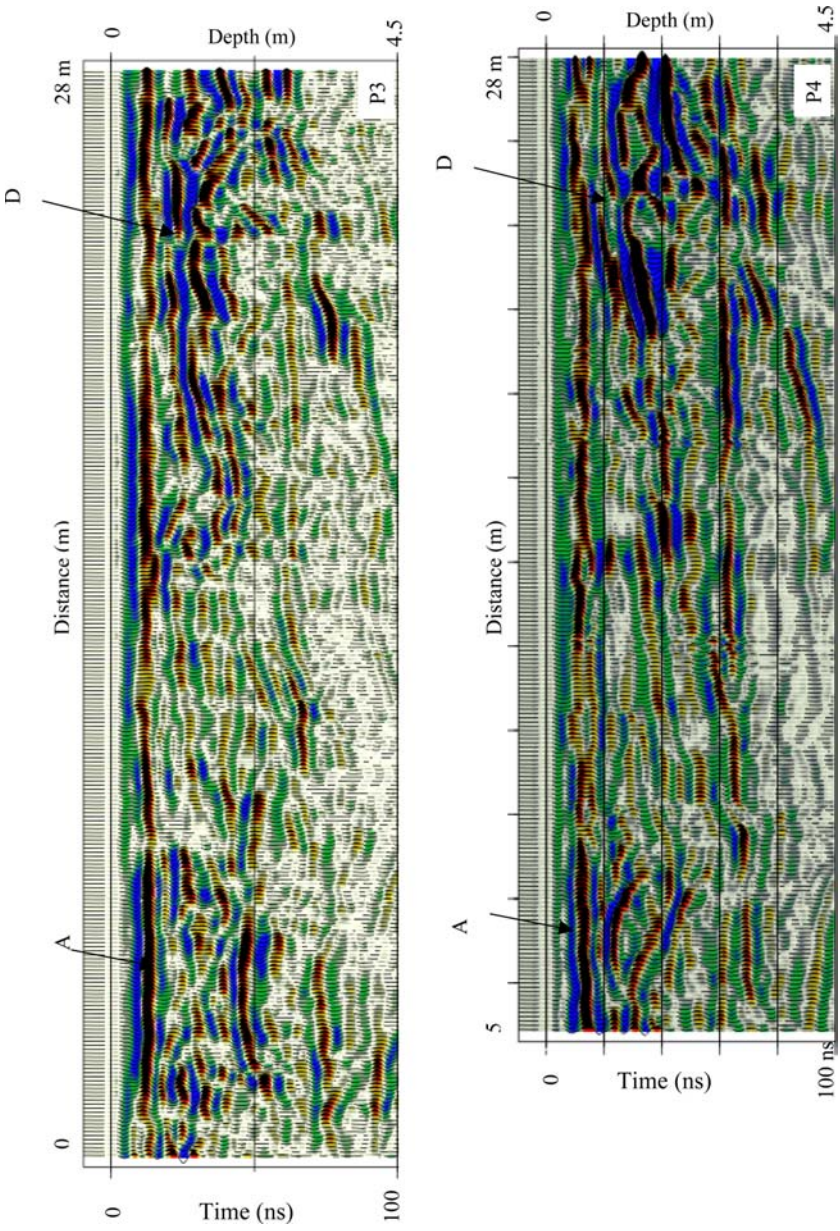

Figure 7. Unmigrated georadar profiles. For locations see Figure 5. The main anomalies are indicated with capital letters.

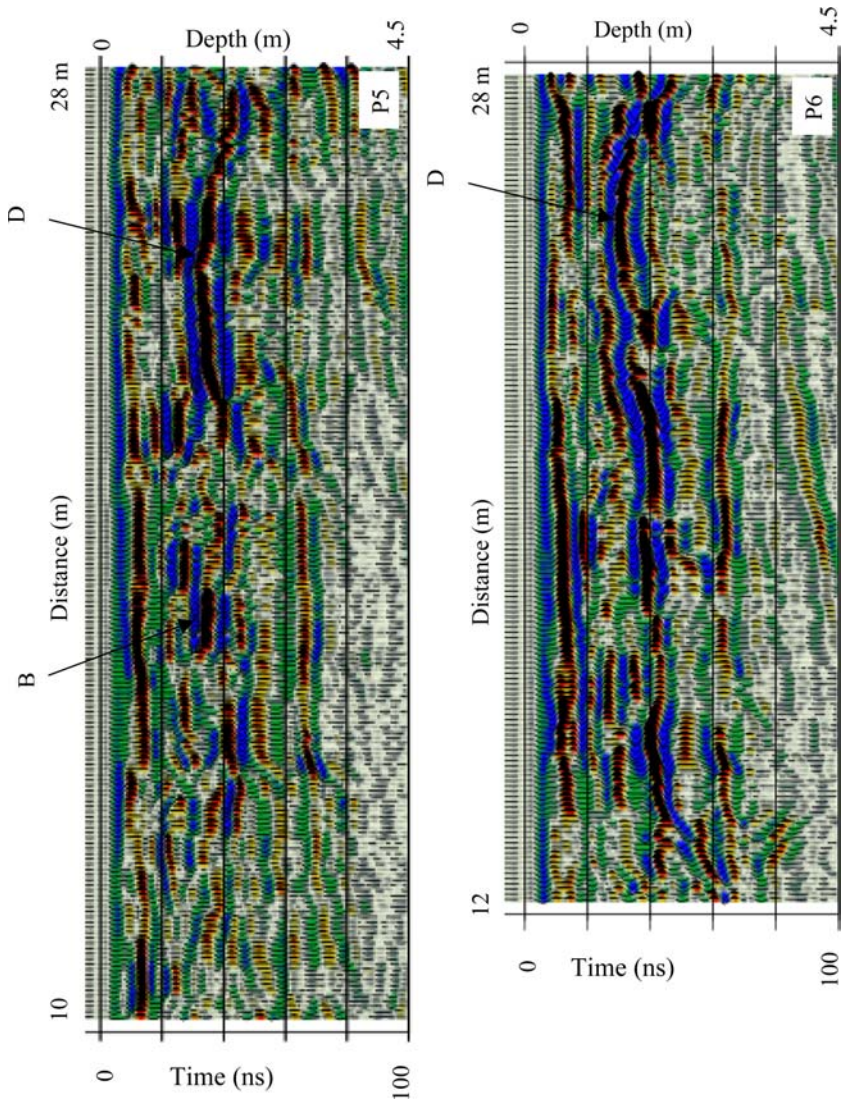

Figure 8. Unmigrated georadar profiles. For location see Figure 5. The main anomalies are indicate with capital letters.

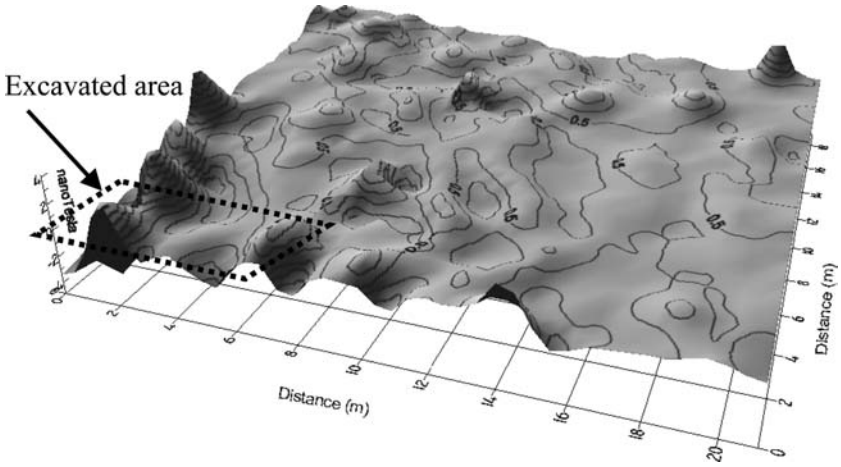

Figure 9. Magnetic gradient after despiking and circular weighted spatial filter. The main anomalies are circular.

that can produce clutters in the georadar and electrical tomography data, the anomalies detected with the electrical tomography and georadar methods can only in part, be carried by anthropogenic activity. The magnetic method was the most sensitive to the anthropogenic structure in this specific case. Therefore the excavation test was located where the overlapping of the anomalies obtained from the three different methods occurred (indicated with 1 in Fig. 2).

3.2.1. Excavation Test

Based on the results obtained from the geophysical surveys, a square test area, 5×5 m wide, was excavated (Fig. 9). The excavation showed a concrete layer about 0.20 m thick below a few centimeters of humus, which we were not able to date. The concrete layer has an irregular surface. A child skeleton was found near the excavated silos, in a man-made hollow. Outside the concrete an anthropogenic-cemented surface was detected. Into and outside the concrete, medieval silos dated to earlier then the XIV century was detected. The silos, having a cylindrical shape of about 1 m of diameter and 1.5 m high, are filled with debris containing earthenware remains. The silos, excavated into sandy and gravel formation were used during the Middle Age to store corn. With abandonment, stones, clay and earthenware remains have filled the silos. Paint on the earthenware remains allowed dating of the silos.

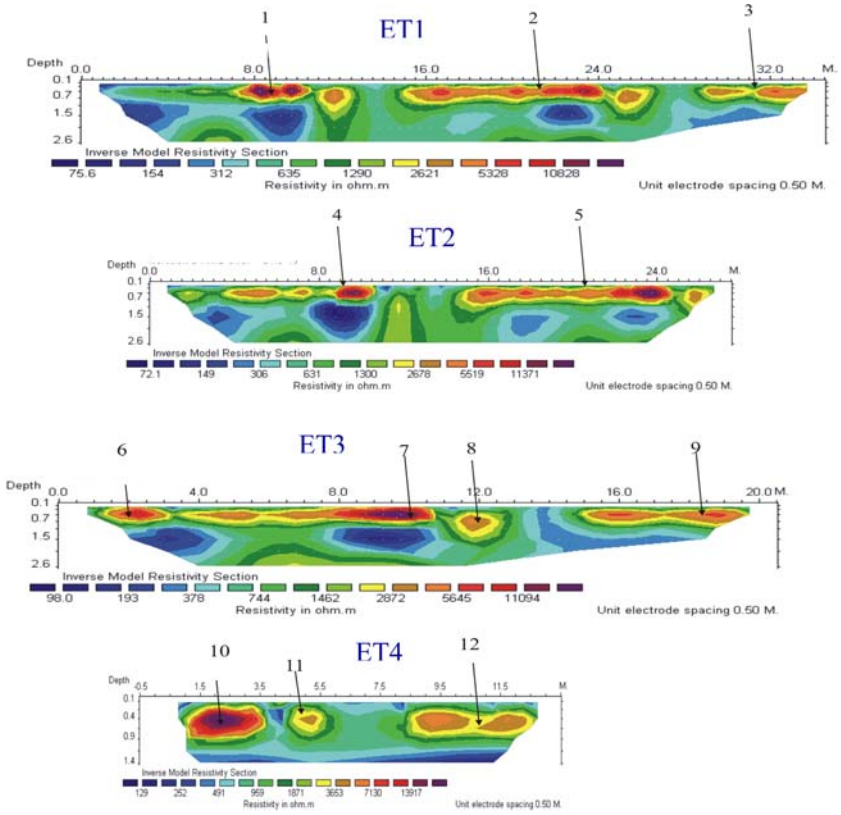

Figure 10. 2D electrical tomography. The profile locations are shown in Figure 2.

3.2.2. Joint Interpretation of Geophysical and Archaeological Data

Comparing the results of excavation with the geophysical data, we can correlate the magnetic anomalies with the earthenware remains within the debris filling the silos, and the resistive layer with the concrete and with the anthropogenic surface located at few decimeters from the topographic level. If we analyze the georadar vertical sections crossing the excavated area (two sections in Fig. 11b,c, located as in Fig. 11a) we observe that the top of the concrete and the silos are detected by georadar. The detailed time slices at 10, 13 and 18 ns, in which the excavated area falls (Fig. 11 a–c), show the limits of the concrete and the location of the silos very well. In detail, the red zone on the corner of the time slices at 10 ns represent the limit of the concrete and the circular anomalies are

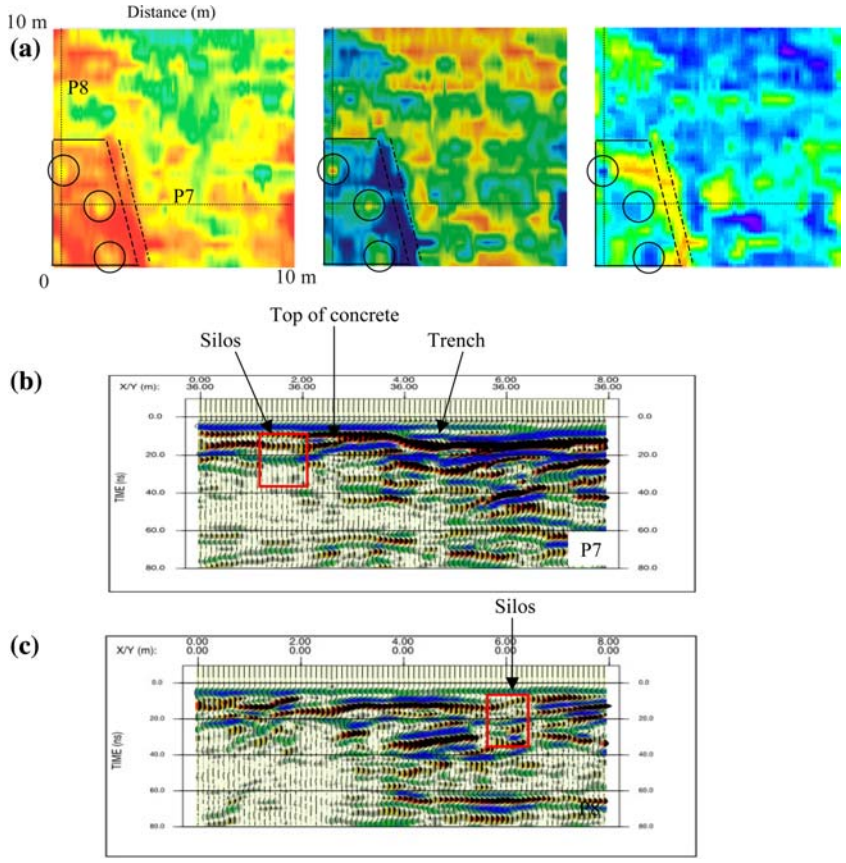

Figure 11. (a) Time slices at 10 ns (on the left), 13 ns (on the center) and 18 ns on the right of the excavated area. The continuous lines indicate the edge of the concrete, the dashed lines the trench, the circles the silos and the dotted lines the location of radar profiles shown in (b) and (c). (b) W–E georadar section labeled with P7 in Figure 11a. S–N georadar section labeled with P7 in Figure 11a.

the silos. Below the concrete (time slice on the right) a semicircular yellow anomaly is present; which can be correlated with a water trench on the boundary of concrete.

The comparison of the geophysical data with the excavation results shows that the anomalies can be referred to different elements of the same structures, i.e., the magnetic methods detected the earthenware ruins while the georadar detected the geometry of the silos. It is interesting to note that in this case the magnetic anomalies are mainly related to the medieval

activities. We speculate that probably the deeper anomalies detected by georadar are diamagnetic, because all the magnetic anomalies detected in the area have a circular shape (Fig. 9) like that produced by silos which are located in the surficial zone.

4. Conclusion

In this study, several geophysical methods were applied to constrain the ambiguity in the reconstruction of a complex archaeological site. The complexity of the study area is due both to geological setting and to the poorly preserved structures. On the basis of the physical characteristics of the sediments and the archaeological ruins the georadar, magnetic and electrical tomography was evaluated to be the best tools to use. The anomalies detected by georadar were not easy to interpret because inhomogeneous material including cemented blocks formed the sediments and the structures are not well preserved. Because the georadar anomalies on the time slices have an irregular shape and a low lateral continuity, it was necessary interpret the data using the time slices and the vertical unmigrated and migrated profiles. The diamagnetic character of the sediments and the presence of earthenware remains suggested the use of the magnetic method which allowed to detect the anthropogenic structures. The electrical tomography was a useful tool to separate the conductive to the resistive anomalies. The joint interpretation of magnetic, electrical tomography and georadar data have given overlapping of anomalies in some places (zones 1 and 2 in Fig. 2) and not in the others. This occurs because the geophysical methods are based on different physical characteristics. Therefore they can detect different bodies with a different degree of resolution.

On the bases of the geophysical results an area (5×5 m wide) was excavated where magnetic, electric and georadar anomalies were overlapped. The excavation test showed a concrete layer about 0.2 m thick and some silos that in the Middle Age were used to store the corn. The silos were filled by debris and earthenware, which produced the magnetic anomalies.

The correlation of the excavation with the geophysical anomalies has shown that the georadar time slices in the geo-archaeological complex area are able to detect anomalies as small as silos 1 m in diameter. The magnetic method has detected small objects like earthenware remains and indirectly has allowed the detection of the silos. The electrical tomography has allowed the detection of the anthropogenic layer few centimeter deep. These results demonstrate that because different methods can detect different objects not always we can apply a joint inversion of the data to improve the consistency of the interpretation. In these cases it is best to apply a joint interpretation of the data.

Acknowledgments

The Author thanks Prof. M. Bernabini and Dr. Steven Arcone for their technical support. This study was partially funded from the ‘Cmmune di Guardiagrele.

References

1. Basile, V., Carrozzo, M.T., Negri, S., Nuzzo, L., Quarta, T., and Villani, A., 2000, A ground-penetrating radar survey for archaeological investigations in an urban area (Lecce, Italy). J. Appl. Geophys., v. 44, no. 1, p. 15–32.
2. Malagodi, S., Orlando, L., Piro, S., and Rosso, F., 1996, Location of archaeological structures using GPR method. Three-Dimensional data acquisition and radar signal processing. Archaeol. Prospect., v. 3, p. 13–23.
3. Piro, S., Goodman, D., and Nishimura, Y., 2000. High-resolution geophysical surveys for the study and characterisation of Traiano’s Villa (Altopiani di Arcinazzo, Roma). 25th general assembly Geophysical Research Abstracts, 2, European Geophysical Society.
4. Whiting, B.M., McFarland, D., Douglas, P., and Hackenberger, S., 2000, Preliminary results of three-dimensional GPR-based study of a prehistoric site in Barbados, West Indies. SPIE Proc. Ser., v. 4084, p. 260–267.
5. Whiting, B.M., McFarland, D.P., and Hackenberger, S., 2002, Three-dimensional GPR study of a prehistoric site in Barbados, West Indies. J. Appl. Geophys., v. 47, no. 3–4, p. 217–226.
6. Piro, S., Goodman, D., and Nishimura, Y., 2002, The location of Emperor Traiano’s villa altopiani di Arcinazzo-Roma) using high-resolution GPR surveys. Bollettino di Geofisica Teorica ed Applicata, v. 43, p. 143–155.
7. Dabas, M., Camerlynck, C., and Freixas, C., 2000, Simultaneous use of electrostatic quadripole and GPR in urban context; investigation of the basement of the Cathedral of Girona (Catalunya, Spain). Geophysics, v. 65, no. 2, p. 526–532.
8. Shaaban, F.F. and Shaaban, F.A., 2001, Use of two-dimensional electric resistivity and ground penetrating radar for archaeological prospecting at the ancient capital of Egypt. J. Afri. Earth Sci., v. 33, no. 3–4, p. 661–671.
9. Dobroka, M., Bernabini, M., Cardarelli, E., and de Nardis, R., 1999, A quasi 2D joint inversion of seismic and geoelectric data. Extended Abstract 61th Conference of EAEG in Helsinky.
10. Loke, M.H. and Baker, R.D., 1996. Rapid least squares inversions of apparent resistivity pseudosections by a quasi-newton method. Geophys. Prospect., v. 44, p. 131–152.
11. Lualdi, M. and Zanzi, L., 2003. 3D GPR investigations on building elements using the PSG: Proc. SAGEEP 2003, April 6–10, San Antonio, TX, USA, p. 803–812.